Dynamic friction modelling without drift and its application in the simulation of a valve controlled hydraulic cylinder system.

Junhong Yang[1], Andrew Plummer[2], Yong Xue[1]

[1]*School of Mechatronics Engineering and Automation, National University of Defense Technology, Changsha, China*

[2]*Centre for Power Transmission and Motion Control, Department of Mechanical Engineering, University of Bath, Bath BA2 5DR, UK*

The full correspondence details for the corresponding author, Junhong Yang. Tel:0086-731-84535584; E-mail addresses: yangjunhong@nudt.edu.cn

Junhong Yang received the B.S. degree from Xi'an Jiaotong University in Xi'an and the M.S. and PH.D. degrees from National University of Defence Technology in Changsha. He is currently a lecture in School of Mechatronics Engineering & Automation at the National University of Defence Technology. Dr. Yang's researches include robotics, high efficient hydraulic diving system for mobile robot, and portable fluid power source.

Andrew Plummer received his PH.D degree from the University of Bath in 1991. He currently is the professor and director of the centre for Power Transmission and Motion Control at the University of Bath. He has a variety of research interests in the field of motion and force control, including inverse-model based control of electrohydraulic servo systems, control of parallel kinematic mechanisms, hybrid hydraulic / piezoelectric actuation, and active vehicle control.

Yong Xue received the B.S. and M.S. degrees from National University of Defence Technology in Changsha. He is currently a Ph.D. student in Mechatronics Engineering & Automation at the National University of Defence Technology. Mr.Xue's research interests include design of robotic mechanism and high efficient hydraulic diving system for mobile robot.

Abstract: The frictional modelling literature is reviewed, and it is demonstrated that unrealistic drift results when the shape coefficient is 1.0 for the LuGre and the Ferretti friction models. Drift will not occur but other dynamic friction characteristics can't be represented when the shape coefficient is 0. Based on the above, the LuGre friction model and the Ferretti friction model are improved. The velocity-friction characteristic, the stick-slip and the cycling caused by friction, and the drift are compared in simulation. The results show that the improved friction model well reflects realistic friction dynamic characteristics and avoids drift. Finally, the improved friction model is used in a nonlinear mathematic model of a valve controlled hydraulic cylinder system. The cylinder's motion at low velocity is simulated and the related experimental results are presented. The results show that the improved friction model gives realistic low velocity motion of the cylinder.

Keywords: friction model; stick-slip; limit cycles; drift; valve controlled cylinder

1. Introduction

Friction is inevitable in mechanical systems. The nonlinear behaviour caused by friction has an adverse influence on the ultra-low velocity and high precision position control of servo mechanisms and hydraulic systems. Friction severely affects the stability of the control system designed to obtain very small steady-state error and could lead to limit cycles and stick-slip, and affect the frequency response bandwidth of the closed loop system [1, 2].

It is important to establish an accurate friction model for both understanding the friction phenomenon and compensating for friction. Until now, a lot of research on friction modelling has been undertaken [3-22]. Many experiments on friction show that there exist two friction regimes [8]: the pre-sliding regime and the sliding regime. In the pre-sliding regime the friction force appears to be a function of relative micro-

displacement (elastic deformation and plastic deformation), and its characteristics are similar to a nonlinear spring. As the displacement becomes larger, the "spring" suddenly ruptures leading to the relative motion between two contact surfaces, and the sliding regime begins. In the sliding regime the friction force appears to be a function of relative velocity.

Up to now, many friction models have been proposed, and they can be classified into two categories: static friction models and dynamic friction models. Among static friction models the representatives are the Coulomb plus viscous friction model [9] and the exponential friction model [10], these models can't predict dynamic friction. Though the seven parameters model [11-12] can reflect the friction's static and dynamic characteristics, in essence it is only the crude combination of static and dynamic models and has no explicit physical content, and moreover it contains redundant parameters. The dynamic friction models include: the Dahl model [13-15], the LuGre model [16], the Elastic-Plastic model [17,18], the Ferretti model [19], the Leuven model [20], and the GMS model [22].

2. The development of dynamic friction modelling

2.1 Dahl friction model

The Dahl model, which was developed in the late 1950s, is a dynamic model with one state, and is widely used to simulate aerospace systems [13, 14]. The Dahl dynamic model essentially describes the friction's pre-sliding regime, and in this regime the friction force is the function of relative micro-displacement between two friction surfaces. The mathematic expression of the Dahl model is as follows [13].

$$\frac{df_{\mathrm{f}}}{dx} = \sigma_0 (1 - \frac{f_{\mathrm{f}}}{f_{\mathrm{c}}} \mathrm{sgn}(v))^{\alpha} \tag{1}$$

Where f_{f} is the friction force, x is the relative micro-displacement between two friction

surfaces, σ_0 is the stiffness coefficient, f_c is the Coulomb friction force, v is the relative velocity of two friction surfaces, α is the coefficient determining the shape of the curve between friction force and relative micro-displacement and is always larger than zero.

Let $v = dx/dt$, $z = f_f/\sigma_0$, and the friction force can be expressed as equation (2) when $\alpha = 1$.

$$\frac{dz}{dt} = v - |v|\frac{\sigma_0 z}{f_c} \tag{2a}$$

$$f_f = \sigma_0 z \tag{2b}$$

2.2 LuGre friction model

The Dahl dynamic model does not take into account the friction's sliding regime. In the sliding regime the lubricant film plays a dominant pole, and it is appropriate to describe the friction force as a function of relative velocity between two friction surfaces. In the case that the velocity is very low, the lubricant film isn't formed fully, and the friction force would decreased when the relative velocity increases, as per the Stribeck phenomenon. The Stribeck phenomenon can be described by the following equation:

$$f_f = \mathrm{sgn}(v)g(v) \tag{3a}$$

$$g(v) = f_c + (f_s - f_c)\exp[-(|v|/v_s)^{\delta_s}] \tag{3b}$$

Where f_s is the maximum static friction force, f_c is the Coulomb friction force, v is the relative velocity of two friction surfaces, v_s is the velocity at the turning point of Stribeck curve, and δ_s is the corrective coefficient of curve.

The literature [16] integrates the Dahl model (2) and the Stribeck equation (3) to derive the following LuGre friction model:

$$\frac{dz}{dt} = v - |v|\frac{\sigma_0 z}{g(v)} \tag{4a}$$

$$g(v) = f_c + (f_s - f_c)\exp[-(v/v_s)^2] \tag{4b}$$

$$f_f = \sigma_0 z + \sigma_1 \frac{dz}{dt} + \sigma_2 v \tag{4c}$$

Where f_f is the total friction force, f_c is the Coulomb friction force, f_s is the maximum static friction force, v is the relative velocity of two friction surfaces, v_s is the velocity at the turning point of Stribeck curve, σ_0 is the equivalent stiffness coefficient between the friction force and the relative displacement of two friction surfaces when the relative velocity's direction changes, σ_1 is the micro-viscous friction coefficient, and σ_2 is the viscous friction coefficient.

2.3 Elastic-plastic friction model

The LuGre model produces steady-state drift when a tiny external vibratory stimulation is applied [17], whereas in practice there isn't relative motion between two the friction surfaces because the vibratory stimulation is smaller than the maximum breakout friction. In the same case, though steady-state drift doesn't arise in the Karnopp friction model, micro-displacement which should arise does not. Based on the above problem, [17] and [18] propose the elastic-plastic friction model as a development of the LuGre friction model.

$$\frac{dz}{dt} = v - \alpha(z,v)v\frac{\sigma_0 z}{g(v)} \tag{5a}$$

$$g(v) = f_c + (f_s - f_c)\exp[-(v/v_s)^2] \tag{5b}$$

$$f_f = \sigma_0 z + \sigma_1 \frac{dz}{dt} + \sigma_2 v \tag{5c}$$

$$\alpha(z,v) = \begin{cases} 0, \ if\ |z| \le z_{ba}\ or\ \mathrm{sgn}(v) \ne \mathrm{sgn}(z) \\ 1, if\ |z| \ge z_{ss}(v) \\ else\ \frac{1}{2}\sin(\pi \frac{z - (\frac{z_{ba} + z_{ss}}{2})}{z_{ss} - z_{ba}}) + \frac{1}{2} \end{cases} \tag{5d}$$

Where f_f, f_c, f_s, v, v_s, σ_0, σ_1, σ_2 are the same as the parameters in the LuGre friction model shown in section 2.2.

$$0 < z_{ba} < z_{ss}(v) \tag{6}$$

$$z_{ss}(v) = \left| g(v)/\sigma_0 \right|_{max} = f_s/\sigma_0 \tag{7}$$

where z_{ba} represents the range of friction state variable z when friction is characterized by linear damping and a linear spring, and z_{ss} represents the range of friction state variable z when the friction contact surface is in the pre-sliding regime in which there are only elastic deformation and plastic deformation.

2.4 The Ferretti Model

Ferretti proposes an integral friction model [19], and the simulation results show that the model is consistent with the LuGre model in terms of reflecting stick-slip, limit cycles, and so on, while being computationally more efficient and avoiding non-physical drift through letting α=0 in the Dahl model. The integral friction model is given in the following.

$$f_f = f_p + f_v + f_z \tag{8a}$$

$$\frac{df_p}{dx} = \sigma_0 (1 - \frac{f_p}{f_s} \mathrm{sgn}(v))^{\alpha} \tag{8b}$$

$$f_v = \mathrm{sgn}(v)(f_s - f_c)\left\{ \exp\left[-\left(|v|/v_s \right)^{\delta_s} \right] - 1 \right\} + \sigma_2 v \tag{8c}$$

$$f_z = \sigma_1 (1 - \mathrm{sgn}(v) \frac{f_p}{f_s})^{\alpha} v \tag{8d}$$

Where f_p is the term which relates friction to micro-displacement in the pre-sliding regime, f_v is the term which relates friction to velocity in the sliding regime, and f_z is the micro-viscous friction term when friction transitions from the pre-sliding regime to

the sliding regime, and the other parameters are the same as the parameters in the LuGre model shown in section 2.2.

2.5 Leuven friction model

In [20], the pre-sliding regime friction force is modelled as a hysteresis function of relative micro-displacement, with nonlocal memory. Considering this factor, it corrects the LuGre model and derives the Leuven friction model.

$$\frac{dz}{dt} = v(1 - \mathrm{sgn}(\frac{f_h(z)}{g(v)})\left|\frac{f_h(z)}{g(v)}\right|^{\delta_1}) \tag{9a}$$

$$g(v) = f_c + (f_s - f_c)\exp[-(|v|/v_s)^{\delta_s}] \tag{9b}$$

$$f_f = f_h(z) + \sigma_1 \frac{dz}{dt} + \sigma_2 v \tag{9c}$$

Where $f_h(z)$ is the hysteresis function with non-local memory, and it is the point symmetrical and strictly increasing function with the input state variable z. $f_h(z)$ can be found by experimental identification[20] or by theoretical modelling[21]. δ_1 is similar to the shape coefficient α in the Dahl model (1). The other parameters are the same as the parameters in the LuGre model shown in section 2.2.

2.6 GMS (Generalized Maxwell-Slip) friction model

The literature [8, 22] takes into account advantages and disadvantages of the elastic-plastic friction model and the Leuven friction model and proposes the GMS friction model. It can not only reflect the non-local memory hysteresis loops and the Stribeck phenomenon in the pre-sliding regime, but also avoid the same steady drift as the elastic-plastic model.

$$f_f = \sum_{i=1}^{N} f_i + \sigma_2 v \tag{10a}$$

$$\frac{df_{\mathrm{i}}}{d\mathrm{t}}=\begin{cases}k_{\mathrm{i}}v & if\ \ f_{\mathrm{i}}\le\alpha_{\mathrm{i}}g(v)\\ \mathrm{sgn}(v)C(\alpha_{\mathrm{i}}-\dfrac{F_{\mathrm{i}}}{g(v)}) & else\end{cases} \tag{10b}$$

$$g(v)=f_{\mathrm{c}}+(f_{\mathrm{s}}-f_{\mathrm{c}})\exp[-(|v|/v_{\mathrm{s}})^{\delta_s}] \tag{10c}$$

Where N is the number of friction model units, k_{i} is the contact stiffness, α_{i} is the split coefficient of the friction model, C is the coefficient concerning the velocity v, f_{i} is the friction force unit, σ_2 is the viscous friction coefficient , and f_{f} is the total friction force. The other parameters are the same as the parameters in the LuGre model shown in section 2.2.

3. Improvement of the LuGre friction model and the Ferretti friction model

Though the elastic-plastic model, the Leuven model and the GMS model can accurately reflect the friction's dynamic characteristics, they are complex. And so it is very difficult to utilize them in closed loop control system analysis and design. Most of the literature about friction for control purpose has adopted the LuGre friction model [23-25]. The literature [15] indicates by simulation that the Ferretti friction model has the same characteristics as the LuGre friction model, and also it is computationally more efficient.

The Ferretti friction model can avoid unrealistic drift when α=0 [15], while the LuGre friction model and the Ferretti friction model can't accurately reflect the friction's dynamic characteristics. The difference in the friction force as a function of velocity is shown in figure 1 and figure 2 when α=0 and α=1, and it is found that the friction model can fully reflect the friction's dynamic characteristics when α=1, but can't reflect the friction's dynamic characteristics when α=0.

Through the above summary of the literature, the following conclusion can be reached: (1) the drift of the friction model mainly occurs in the pre-sliding regime in

which there is no obvious relative motion in reality, and furthermore, the drift mainly occurs in the elastic deformation stage of the pre-sliding regime; (2) the basis of the LuGre friction model and Ferretti friction model is the Dahl friction model, and the parameter α of the Dahl friction model is the coefficient determining the shape of curve between friction force and relative micro-displacement in the pre-sliding regime; (3) when α=0, drift can be avoided, and when α=1, the friction's dynamic characteristics can be well reflected.

Therefore the following improvement of the LuGre and the Ferretti friction models is derived. The friction process is divided into the two stages. The first stage is the elastic deformation, in which the friction force is not larger than the coulomb friction force f_c, and by letting α=0 in this stage drift is avoided. The second stage is the plastic deformation and sliding friction, and by letting α=1 in this stage ensures the friction's dynamic characteristics are modelled correctly.

3.1 The improved LuGre friction model

$$\frac{dz}{dt} = v(1 - \frac{\sigma_0 z}{g(v)}\mathrm{sgn}(v))^{\alpha} \tag{11a}$$

$$g(v) = f_c + (f_s - f_c)\exp[-(v/v_s)^{\delta_s}] \tag{11b}$$

$$f_f = \sigma_0 z + \sigma_1 \frac{dz}{dt} + \sigma_2 v \tag{11c}$$

$$\alpha = \begin{cases} 0 & |z| \le z_{es} \\ 1 & |z| > z_{es} \end{cases} \tag{11d}$$

Where $z_{es} = f_c / \sigma_0$, f_c is the coulomb friction force, σ_0 is the stiffness coefficient. The term z_{es} represents the range of friction state variable z when the friction contact surface is in the pre-sliding regime in which there is only elastic deformation.

3.2 The improved Ferretti friction model

$$f_{\mathrm{f}} = f_{\mathrm{p}} + f_{\mathrm{v}} + f_{\mathrm{z}} \tag{12a}$$

$$\frac{df_{\mathrm{p}}}{dx} = \sigma_0 (1 - \frac{f_{\mathrm{p}}}{f_{\mathrm{s}}} \mathrm{sgn}(v))^{\alpha} \tag{12b}$$

$$f_{\mathrm{v}} = \mathrm{sgn}(v)\left(f_{\mathrm{s}} - f_{\mathrm{c}}\right)\left\{ \exp\left[-\left(|v|/v_{\mathrm{s}}\right)^{\delta_{\mathrm{s}}}\right] - 1\right\} + \sigma_2 v \tag{12c}$$

$$f_z = \sigma_1 (1 - \mathrm{sgn}(v) \frac{f_p}{f_s})^{\alpha} v \tag{12d}$$

$$\alpha = \begin{cases} 0 & |f_p| \le f_c \\ 1 & |f_p| > f_c \end{cases} \tag{12e}$$

Where f_{p} is the term which relates friction to micro-displacement in the pre-sliding regime, f_c is the coulomb friction force, and $|f_p| \le f_c$ means that the friction is in the elastic deformation stage and $|f_p| > f_c$ means that the friction is in the plastic deformation and sliding regime.

4. Analysis of simulation experiment

Simulation results [15] already indicate the consistency of the LuGre model and the Ferretti model, and when α=0 both can avoid drift, while through simulation it is found that the model can't reflect stick-slip and limit cycles caused by friction nonlinearity when α=0. For brevity , in the following only results for the Ferretti model and the improved Ferretti model are given, and the simulation parameters which are the same as [15] are shown in table 1.

Table 1. The parameters of friction simulation

σ_0	σ_1	σ_2	f_{c}	f_{s}	v_{s}	δ_{s}
10^5 N/m	$\sqrt{10^5}$ Ns/m	0.4 Ns/m	1N	1.5N	0.004 m/s	2

4.1 Simulation of the relation between the friction force and velocity

Let v=0.001t, set the integrator and let its absolute tolerance equal to 1×10^{-8}, external reset is none, initial condition source is internal, initial condition is zero, and not limit output and not ignore limit and reset when linearizing. When adopting variable simulating step, it is needed to add a two-order filter whose cut off frequency is 10KHz before the derivate of z goes into the equation (11a) when simulating the improved LuGre model, the solver is ode45 (Dormand-Prince), and Relative tolerance is 1e-3. If the fixed simulating step is adopted for the two improved friction models, the simulating step is equal to 0.0001 and the solver is ode3 (Bogacki-Shampine). Separately solving the improved Ferretti model, the Ferretti model (α=1) and the Ferretti model (α=0) gives the curves between the friction force and the relative velocity shown in Figure 1 and Figure 2.

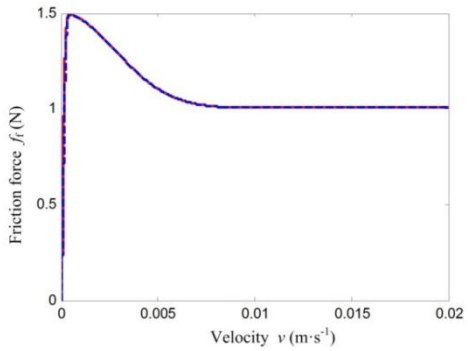

Figure 1. Friction characteristics with varying velocity (dashed line: Ferretti model with α=1，solid line: improved Ferretti model)

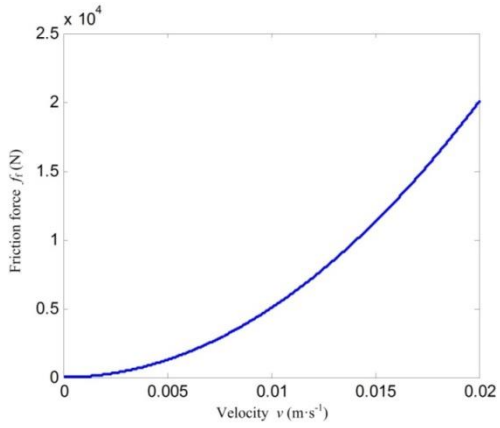

Figure 2. Friction characteristics with varying velocity (Ferretti model with α=0)

The simulation result shows that the friction characteristics reflected by the improved Ferretti model and the Ferretti model with α=1 are very similar.

4.2 Simulation of Stick-slip and Limit Cycles

The simulation of stick-slip adopts the model shown in Figure 3, where the spring stiffness k=2N·m^{-1}, the moving speed of the spring's end is $\bar{v}$ =0.1 m·s^{-1}, m is unit mass, and other simulation parameters are shown in table 1. The stick-slip simulation results are shown in Figure 4 and Figure 5. The dynamic model for simulation is as follows:

$$k\int_0^t(\bar{v}-\dot{x})dt - f_f = m\ddot{x} \qquad (13)$$

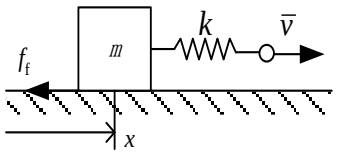

Figure 3. Simulation model for stick-slip and limited cycles

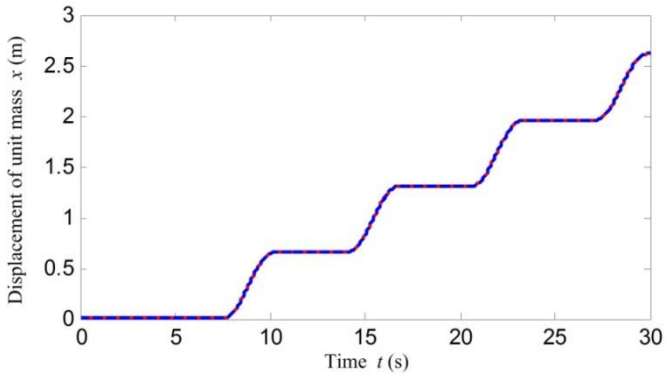

Figure 4. Stick-slip simulation experiment(dashed line: Ferretti model with α=1， solid line: improved Ferretti model)

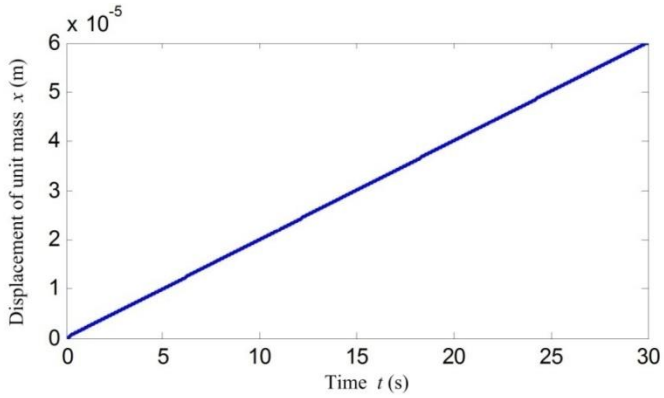

Figure 5. Stick-slip simulation experiment (Ferretti model with α=0)

Figure 6 and Figure 7 show the simulation of a Proportional-Integral-Derivative closed loop position control of the unit mass m (taking out the spring) with friction. The figures show this control system's step response, where the input step reference signal $\bar{x}$ =1m, the output signal is the displacement of unit mass, and the parameters of the PID controller are k_p=3 N·m^{-1}, k_i=4 N·m^{-1}·s^{-1}, k_d=6 N·s·m^{-1}. The dynamic model for simulation is as follows:

$$-k_p(x-\bar{x})-k_i\int(x-\bar{x})dt-k_d\dot{x}-f_f=m\ddot{x} \tag{14}$$

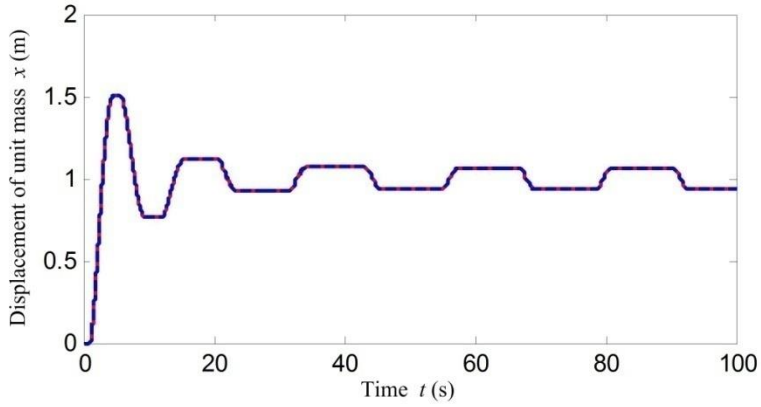

Figure 6. Hunting simulation experiment (dashed line: Ferretti model with α=1， solid line: improved Ferretti model)

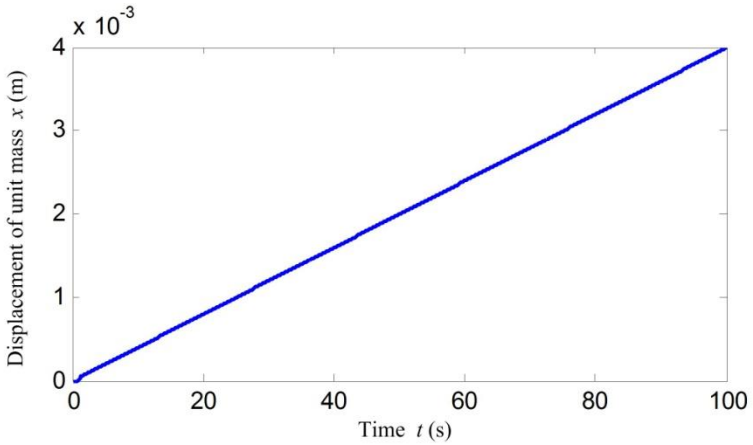

Figure 7. Hunting simulation experiment (Ferretti model with α=0)

The simulation results show that both the improved Ferretti model and the Ferretti model with α=1 can reflect stick-slip and limit cycles caused by friction, while the Ferretti model with α=0 can't reflect these phenomena.

4.3 Simulation of non-physical drift

With a horizontal vibratory stimulation on the unit mass m in Figure 3, and when the maximum of the vibratory stimulation's amplitude doesn't exceed the maximum of breakout friction (the maximum static friction force), in reality the unit mass wouldn't exhibit micro-motion, but when adopting the LuGre friction model or the Ferretti friction model with α=1 in the control system, the simulation result shows that there is a steady drift of the unit mass. In the simulation, the input signal is the imposed external force on the mass, and the output signal is the displacement of unit mass. The imposed external force is $u(t) = a + b\sin(wt)$, where a=0.5 N, b=0.25 N, w=6л/5 rad·s^{-1}. So the maximum external force is 0.75N, and it is samller than the maximum static friction force f_s showed in Table 1. Other parameters are as shown in table 1.

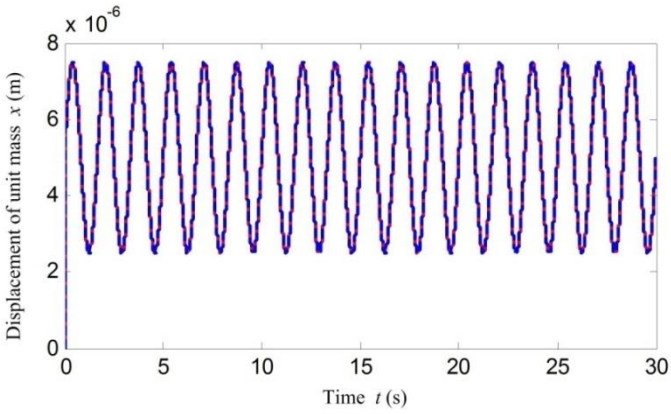

Figure 8. Simulation experiment with external vibration force (dashed line: Ferretti model with α=0，solid line: improved Ferretti model)

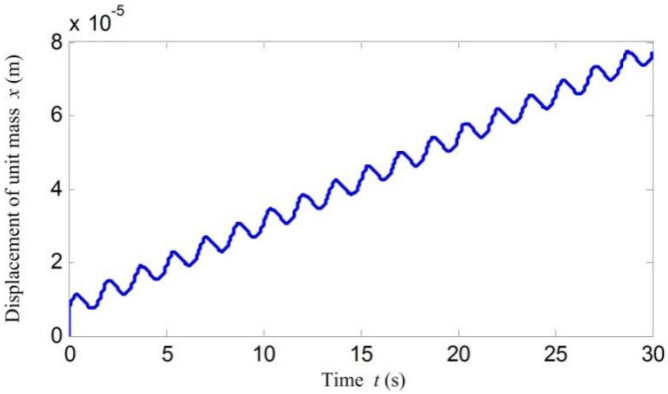

Figure 9. Simulation experiment with external vibration force (Ferretti model with α=1)

The displacements of the unit mass for different friction models are shown in Figure 8 and Figure 9. It can been seen that the Ferretti model with α=1 produces steady drift as showed in Figure 9, and this drift would not occur in reality because the stimulating force is less than the maximum static friction force. Figure 8 shows that both the Ferretti model with α=0 and the improved Ferretti model don't produce the steady drift as showed in Figure 9

From the above results, it can been seen that the improved Ferretti model can reflect the stick-slip and limit cycle phenomena caused by friction, and at the same time avoid drift. The authors have found that the improved LuGre model has the same characteristics as the improved Ferretti model, but results are not included here.

5. Application of the improved LuGre friction model in the simulation of a valve controlled hydraulic cylinder system

Friction nonlinearity in valve controlled hydraulic cylinders degrades the position tracking precision, and can result in limited cycles, stick-slip, and reduces the frequency response bandwidth of the closed loop system [26, 27]. Building a model which can reflect the real dynamic friction characteristic is very useful for simulation analysis and friction compensation control.

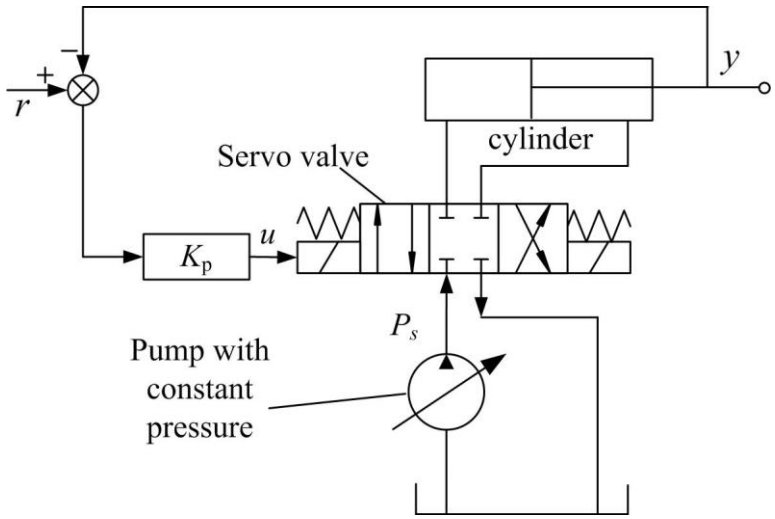

Figure 10. Valve controlled cylinder system

A valve controlled cylinder system is shown in Figure 10. When the friction force is not considered, the plant's nonlinear state space model is given by equation (15) [28], where the state variable x_1 is the displacement of the cylinder y, x_2 is the velocity of the cylinder, x_3 is the pressure of the cylinder rodless chamber, x_4 is the pressure of the cylinder rod chamber, and other parameters is shown in table 2.

$$\begin{cases} \dot{x}_1 = x_2 \\ \dot{x}_2 = \dfrac{A_1}{M}x_3 - \dfrac{B}{M}x_2 - \dfrac{A_2}{M}x_4 - \dfrac{F_L}{M} \\ \dot{x}_3 = g_1(\boldsymbol{x})u - \dfrac{A_1}{V_1}x_2 - \dfrac{C_i}{V_1}(x_3 - x_4) - \dfrac{C_e}{V_1} \\ \dot{x}_4 = g_2(\boldsymbol{x})u + \dfrac{A_2}{V_2}x_2 - \dfrac{C_i}{V_2}(x_4 - x_3) - \dfrac{C_e}{V_2} \end{cases} \tag{15}$$

Where

$$g_1(\boldsymbol{x}) = \mathrm{sgn}((1+\mathrm{sgn}(u))p_s/2 - \mathrm{sgn}(u)x_3) \times \frac{C_d w_3}{V_1}\sqrt{\frac{2}{\rho}\left|((1+\mathrm{sgn}(u))p_s/2 - \mathrm{sgn}(u)x_3)\right|}$$

$$g_2(\boldsymbol{x}) = -\mathrm{sgn}((1-\mathrm{sgn}(u))p_s/2 + \mathrm{sgn}(u)x_4) \times \frac{C_d w_5}{V_1}\sqrt{\frac{2}{\rho}\left|((1-\mathrm{sgn}(u))p_s/2 + \mathrm{sgn}(u)x_4)\right|}$$

When considering friction, the second equation of state space model (15) should be changed into the following equation.

$$\dot{x}_2 = \frac{A_1}{M}x_3 - \frac{B}{M}x_2 - \frac{A_2}{M}x_4 - \frac{F_L}{M} - \frac{f_f}{M}\mathrm{sgn}(x_2) \tag{16}$$

Where f_f is the friction force and can be found through the improved Ferretti friction model.

Firstly, the Coulomb friction force f_c and the maximum static friction force f_s of the improved Ferretti friction model need to be determined experimentally. Lay the cylinder horizontally, and give the servo valve a small opening signal. The piston starts to move at a very small constant velocity. The inertial force caused by the piston rod can be ignored due to the small mass of the piston rod and its very small acceleration. Measure the pressure of the rodless chamber and the rod chamber, and the friction force of the cylinder can be derived by the force balance formula $f_f = p_1 A_1 - p_1 A_2$. The curves in Figure 11 are the friction force and the velocity when the piston rod is extending, and the curves in Figure 12 are the friction force and the velocity when the piston rod is retracting. The dynamic friction characteristic is obvious in figure 11 and not in Figure 12. It can be found in figure 11 that $f_c \approx 100\mathrm{N}$, $f_s \approx 145\mathrm{N}$ and $v_s = 3\times10^{-4} m\cdot s^{-1}$.

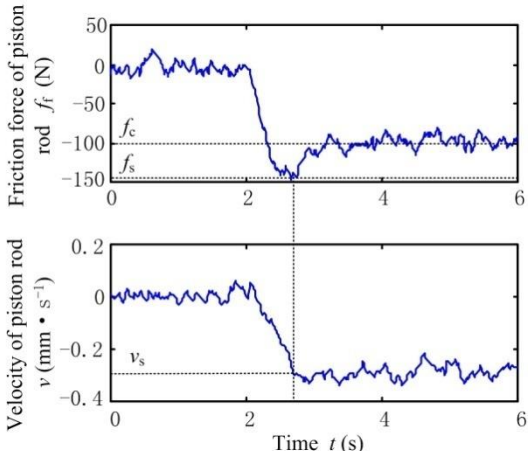

Figure 11. Friction force and velocity when extending

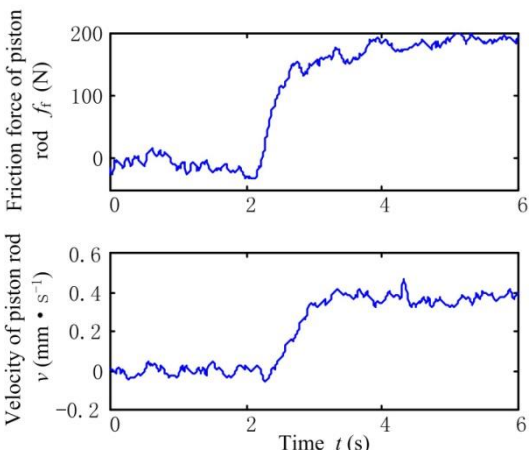

Figure 12. Friction force and velocity when contracting

Table 2. Simulating parameters of valve controlled cylinders

Parameter name		Value	Parameter name		Value
Valve opening area gradient	w_3/m	1.28×10^{-2}	Bulk modulus	K/ MPa	750
Valve opening area gradient	w_5/m	1.28×10^{-2}	Viscous damping coefficient	B/(N • s • m^{-1})	800
Flow coefficient	C_d	0.67	Mass of the piston rod	M /Kg	5
Area of rodless chamber	A_1/ m^2	1.257×10^{-3}	Density	ρ / (kg • m^{-3})	0.875×10^{3}
Area of rod chamber	A_2/ m^2	0.641×10^{-3}	Coefficient of internal leakage	C_i/(m • s^{-1} • Pa^{-1})	3.28×10^{-13}
Initial volume of rodless chamber	V_{10}/m^3	2.665×10^{-4}	Coefficient of external leakage	C_e/(m • s^{-1} • Pa^{-1})	9.10×10^{-13}
Initial volume of rod chamber	V_{20}/m^3	1.709×10^{-4}	Pressure of power source	p_s / MPa	27

Secondly, the equivalent stiffness coefficient σ_0, the micro-viscous friction coefficient σ_1 and the viscous friction coefficient σ_2 need to be determined. Because the viscous friction force has been considered in the second equation of the state space model (15), let σ_2=0. The values of σ_0, σ_1 and δs are from the reference [13]: σ_0=105N • m^{-1}, $\sigma_1=\sqrt{10^5}\,\mathrm{N\cdot s\cdot m^{-1}}$ and δ_s =2. For the closed loop controller, let the commanded displacement of the piston rod be r=0.025sin(6.28t) m, and the proportional position controller is given by u= 0.04(r-y). The output displacement of the piston rod is shown

in Figure 13 and Figure 14. The corresponding experiment is done on the actual valve controlled cylinder system, and the displacement of the cylinder is showed in Figure 15.

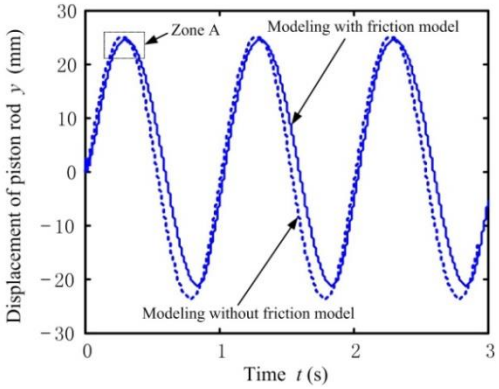

Figure 13. Displacement of the cylinder with friction model

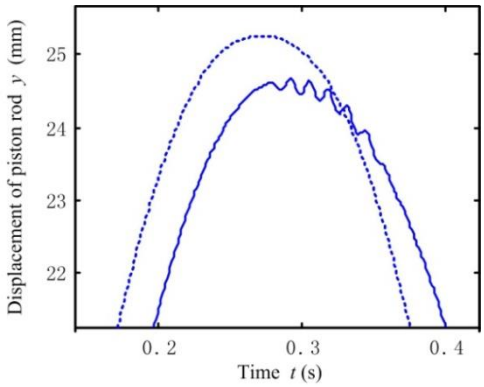

Figure 14. Zoom in on the zone A of Fig.13

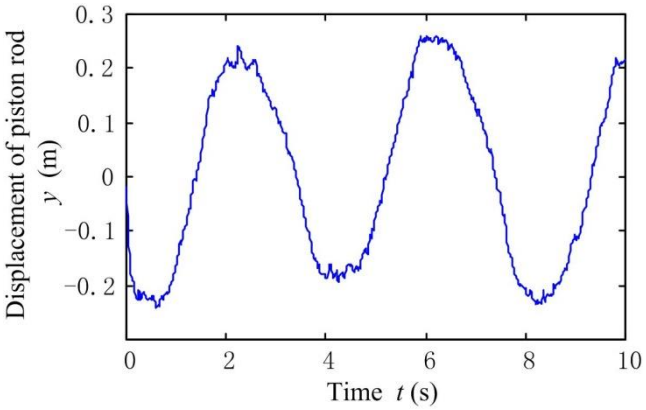

Figure 15. The hunting displacement of the piston rod near zero velocity

Figure 13 and Figure 14 show that the state space model including the improved friction model can reflect the limit cycles when the direction of the piston rod movement changes and its velocity is very small.

Finally, the drift is simulated on the valve controlled cylinder system with the Ferretti friction and with the improved Ferretti friction. The simulation model is shown in Figure 16, and a very small hunting stimulation is exerted on the piston rod through a simple closed loop proportional force control. Let the command force be F_e=40+20sin(6л/5) N , and the actual force exerted on the piston rod is very close to F_e , its maximum value of 60N is less than the Coulomb friction force (100N) and the

maximum static friction force (145N). Because of the sign function and absolute value function in the state space equation (15), there are some high-frequency components in the feedback signal, so a two-order filter with 20 rad/s cut off frequency is added as shown in Figure16. The proportional coefficient is K_p=0.005.

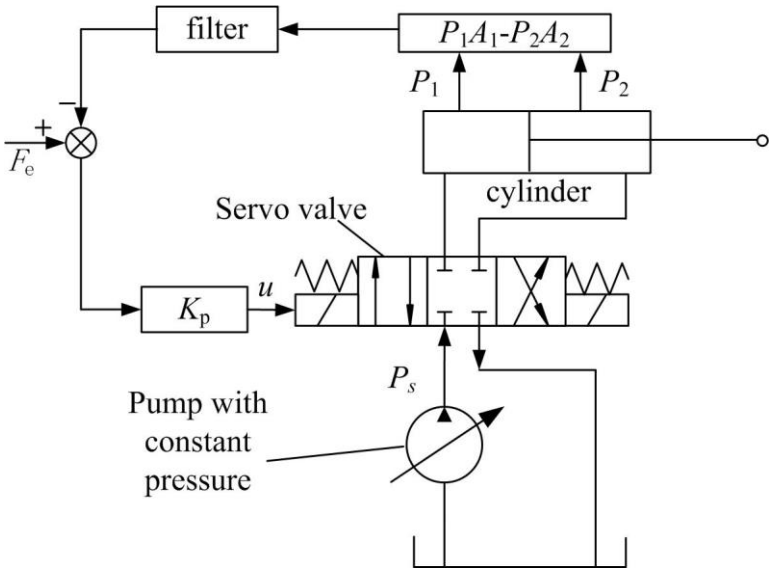

Figure 16. Simulation of the valve controlled hydraulic cylinder system with external vibration force

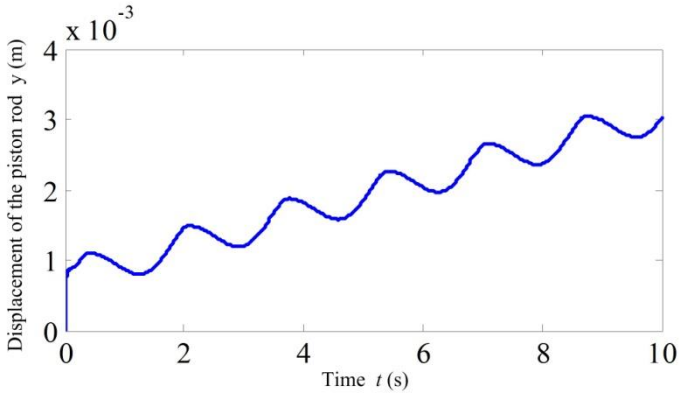

Figure 17. Displacement of the piston rod with the LuGre friction model

Figure 17 shows the displacement of the piston rod when the friction part of equation (16) adopts the Ferretti friction model. This shows that the displacement drifts up over time. In fact, the displacement shouldn't drift up because the force exerted on the piston rod is less than the Coulomb friction force and the maximum static friction force, and so the mathematic model is not correct under this situation.

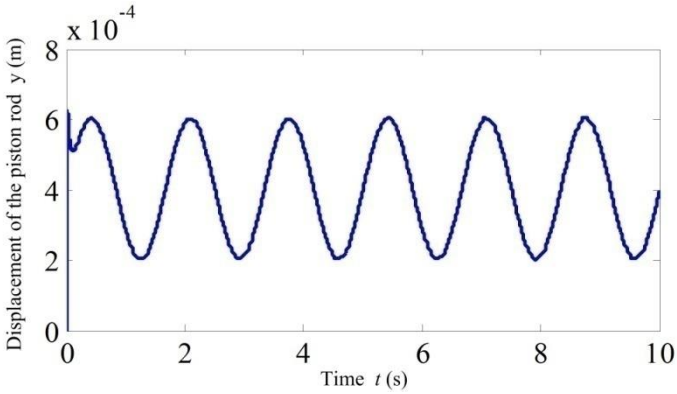

Figure 18. Displacement of the piston rod with the improved LuGre friction model

When adopting the improved friction model, the displacement of the piston rod is shown in Figure18, and no drift occurs.

6. Conclusions

The development process of a dynamic friction model has been systemically summarized, resulting in a friction model which is simple and well reflects the dynamic behaviour of friction in reality.

It was found that the LuGre and Ferretti models can well reflect the friction dynamic characteristics when the coefficient α determining the shape of curve between friction force and relative micro-displacement equals to 1.0, but drift occurs; when α=0, there is no drift in the model, but the friction dynamic characteristics are not well reflected. Therefore in this work the value of α is varied, so that α=0 to avoid drift when friction is in the pre-sliding regime (elastic deformation), and α=1 to reflect sliding friction when friction is in the plastic deformation stage and the sliding regime. The corresponding improved LuGre and Ferretti friction models were developed, and the simulation results show that the improved friction models can well reflect the friction dynamic characteristics and don’t produce drift.

Finally, the improved LuGre friction model was applied to the modelling of a nonlinear valve controlled hydraulic cylinder system, and the related simulation

experiments were done. The results show that the model of the hydraulic system including the improved Ferretti friction model exhibits realistic low velocity friction dynamic characteristics and at the same time doesn't produce drift.

Acknowledgements

This work is supported by the National Natural Science Foundation of China (No.51205400).

References

[1] Friedland B and Park Y J, *On adaptive friction compensation*, IEEE Transaction Automatic Control. 37(1992)37, pp. 1609-1612

[2] Pierre E.Dupont and Eric P.Dunlap, *Friction modelling and PD compensation at very low velocities*, Journal of Dynamic System, Measurement, and Control. 117(1995), pp. 8-14

[3] Susanne V.Krichel and Oliver Sawodny, *Non-linear friction modelling and simulation of long pneumatic transmission lines*, Mathematical and Computer Modelling of Dynamic Systems. 6(2013), pp.1-22

[4] Daniel Helmick and William Messner, *Describing function analysis of Dahl model friction*, 2009 American Control conference. 6(2009), pp.814-819

[5] H. Olsson, K. J. Astrom, C.Canudas de Wit, M. Gafvert, and P. Lischinsky, *Friction models and friction compensation*, European Journal of Control. 4(1998), pp.176-195

[6] A. Bonsignore, G.Ferretti, and G.Magnani, *Analytical formulation of the classical friction model for motion analysis and simulation*, Mathematical and Computer Modelling of Dynamical systems. 5(1)(1999), pp.43-54

[7] C.L. Chen, K. C.Lin, and C. Hsieh, *Presliding friction mode: modelling and experimental study with a ball-screw-driven set-up*, Mathematical and Computer Modelling of Dynamical Systems. 11(4)(2005), pp.397-410

[8] Lampaert V， Al-Bender F, and Swevers J, *A generalized maxwell-slip friction model appropriate for control purposes*, Physics and Control International Conference. (2003), pp.1170-1177

[9] Wei-wei Shang, Shuang Cong, and Shi-long Jiang. *Dynamic model based nonlinear tracking control of a planar parallel manipulator*, Nonlinear Dynamic. 60(4)(2010), pp.597-606

[10] Lorinc Marton, Szabolcs Fodor, and Nariman Sepehri, *A practical method for friction identification in hydraulic actuators*, Mechatronics. 21(2011), pp.350-356

[11] Armstrong B , Dupont P , and Canudas de Wit C, *A survey of models , analysis tools and compensation methods for the control of machines with friction*, Automatica. 30(7)(1994) , pp.1083-1138

[12] EJ Berger, *Friction modelling for dynamic system simulation*, Applied Mechanics Review. 55(6)(2002), pp.535-577

[13] P.R.Dahl, *A solid friction model*, Technical Report TOR-0158(3107-18)-1, The Aerospace Corporation, E1 Segundo, Calif. (1968)

[14] K.J. Astrom and C.Canudas-de-Wit, *Revisiting the LuGre Model*, IEEE Control System Magazine. 28(6)(2008), pp.101-114

[15] Ferretti G, Magnani G.A, and Rocco P, *An integral friction model*, Proceedings of the 2004 IEEE international Conference on Robotics & Automation. (2004), pp.1809-1813

[16] Canudas C and Olsson H, *A new model for control of system with friction*, IEEE Transaction on Automatic Control. 40(3)(1995), pp.419-423

[17] Dupont P, Armstrong B, and Hayward V, *Elasto-plastic friction model: contact compliance and stiction*, Proceeding of the American Control Conference. (2000), pp.1072-1077

[18] Dupont P, Hayward V, Armstrong B, and Altpeter F, *Single state elastoplastic friction models*, IEEE Transaction on Automatic Control. 47(5)(2002), pp.787-792

[19] Gianni Ferretti, Gianantonio Magnani, and Paolo Rocco, *Single and multistate integral friction model*, IEEE Transactions on Automatic Control. 49(12)(2004), pp.2292-2297

[20] Swevers J, Al-Bender F, Ganseman C G, and Projogo T, *An integrated friction model structure with improved presliding behavior for accurate friction compensation, modification of the leuven integrated friction model structure*, IEEE Transaction on Automatic Control. 45(4)(2000), pp.675-686

[21] S.Bjorklund, *A random model for micro-slip between nominally flat surfaces*, ASME J. Tribology. 119(1997), pp.726～732

[22] Michael Ruderman and Torsten Bertram, *Modified maxwell-slip model of presliding friction*, The 18th IFAC World Congress. 8(2011), pp.10764-10769

[23] Khayati Karim, Bigras pascal, and Dessaint Louis-A, *LuGre model-based friction compensation and positioning control for a pneumatic actuator using multi-objective output-feedback control via LMI optimization*, Mechatronics. 19(4)(2009), pp.535-547

[24] Schindele D and Aschemann H. *Adaptive friction compensation based on the LuGre model for a pneumatic rodless cylinder*, Industrial Electronics. 11(2009), pp.1432-1437

[25] Seifabadi Reza, Rezaei Seyed, Ghidary Saeed, and Zareinejad Mohammad, *A teleoperation system for micro positioning with haptic feedback*, International Journal of Control, Automation and System. 11(4)(2013), pp.768-775

[26] Yuan-Jay Wang, *Characterization and quenching of friction-induced limit cycles of electro-hydraulic servovalve control systems with transport delay*, ISA Transactions. 49(2010), pp.489-500

[27] Ying-Jeh Huang and Yuan-Jay Wang, *Limit cycle analysis for electro-hydraulic systems with friction*, Journal of the Chinese Institute of Engineers. 25(3)(2002), pp.277-285

[28] Yang Junhong, Yi Ziqiang, and Li Shengyi, *Nonlinear modelling and feedback linearization of valve controlled asymmetrical cylinder*, Chinese Journal of Mechanical Engineering. 42(5)(2006), pp.203-207